Electronic Supplementary Material (ESI) for Journal of Materials Chemistry A.

Electronic supplementary information

Designing Thickness-Insensitive Cathode Interlayers via Constructing Noncovalently Conformational Locks for Highly Efficient Non-fullerene Organic Solar Cells

Haolan Zheng[a, b], Lin Hu*[a], Xiaotian Hu*[c], Hongxiang Li[d], Jianwei Quan[a, b], Yingzhi Jin[a], Xinxing Yin[a], Jiaxing Song[a], Zhen Su[a], Dan Zhou*[b] and Zaifang Li*[a]

[a] China-Australia Institute for Advanced Materials and Manufacturing (IAMM), Jiaxing University, Jiaxing 314001, China

[b] Key Laboratory of Jiangxi Province for Persistent Pollutants, Control and Resources Recycle, Nanchang Hangkong University, 696 Fenghe South Avenue, Nanchang 330063, China

[c] Institute of Polymers and Energy Chemistry (IPEC)/Jiangxi Provincial Key Laboratory of New Energy Chemistry, Nanchang University, 999 Xuefu Avenue, Nanchang 330031, China.

[d] College of Polymer Science and Engineering, State Key Laboratory of Polymer Materials Engineering, Sichuan University, Chengdu 610065, China

*Corresponding author: hulin@zjxu.edu.cn, happyhu@ncu.edu.cn, zhoudan@nchu.edu.cn, zaifang.li@zjxu.edu.cn

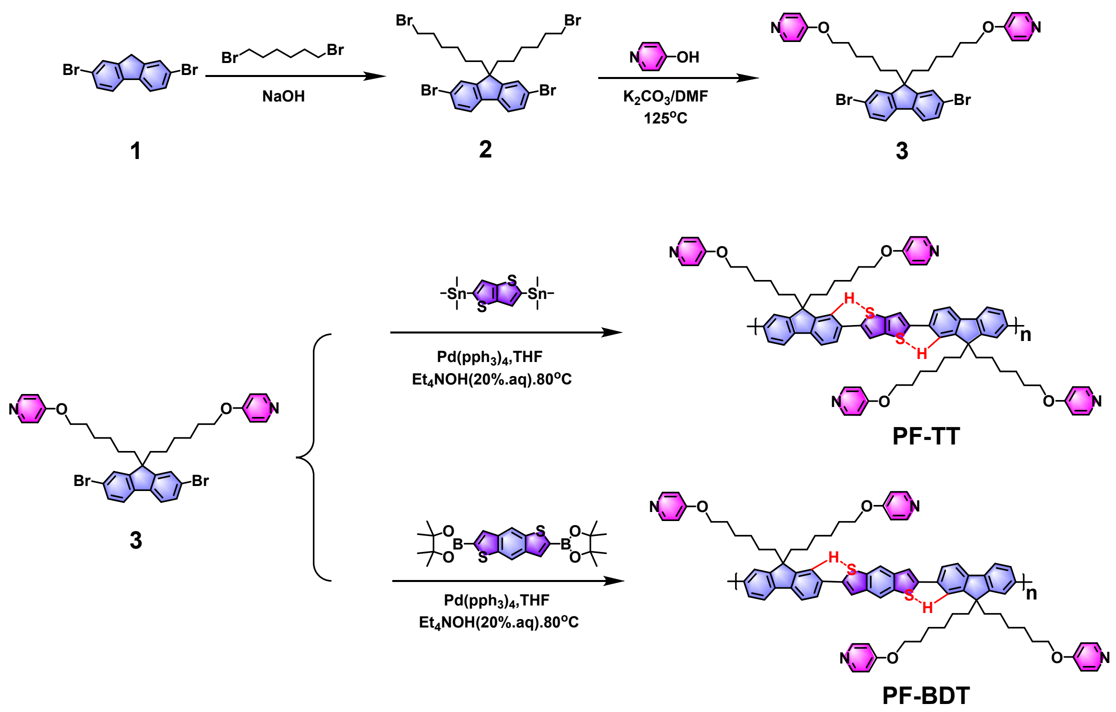

Scheme S1. The synthetic routes of PF-TT and PF-BDT.

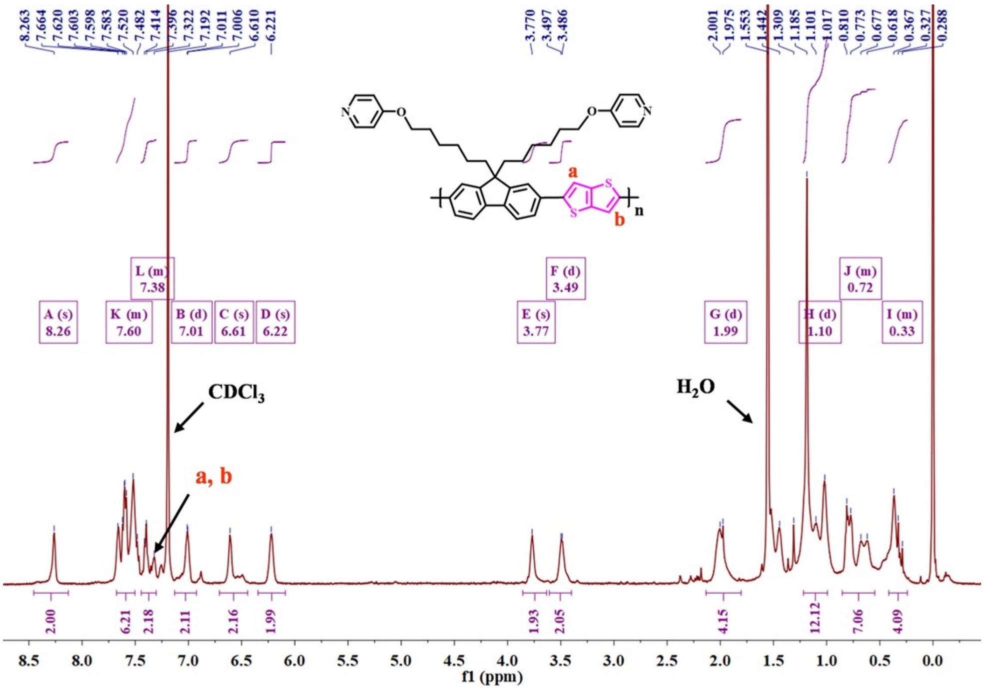

Fig. S1 The ^{1}H NMR spectrum of PF-TT. $CDCl_3$ is used as the deuterium reagent.

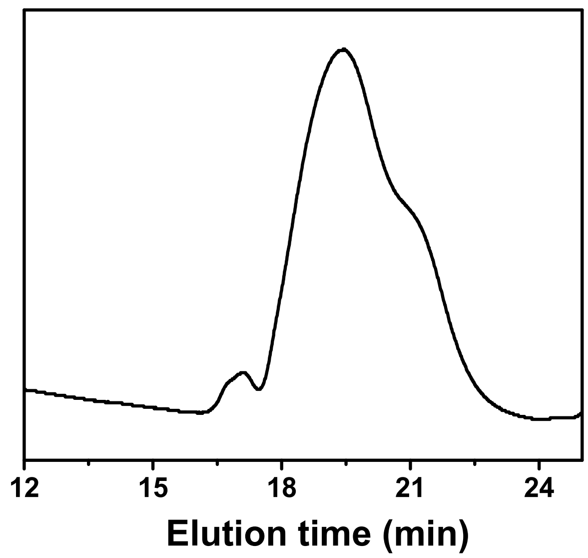

Fig. S2 GPC trace of PF-TT. THF is used as the eluent.

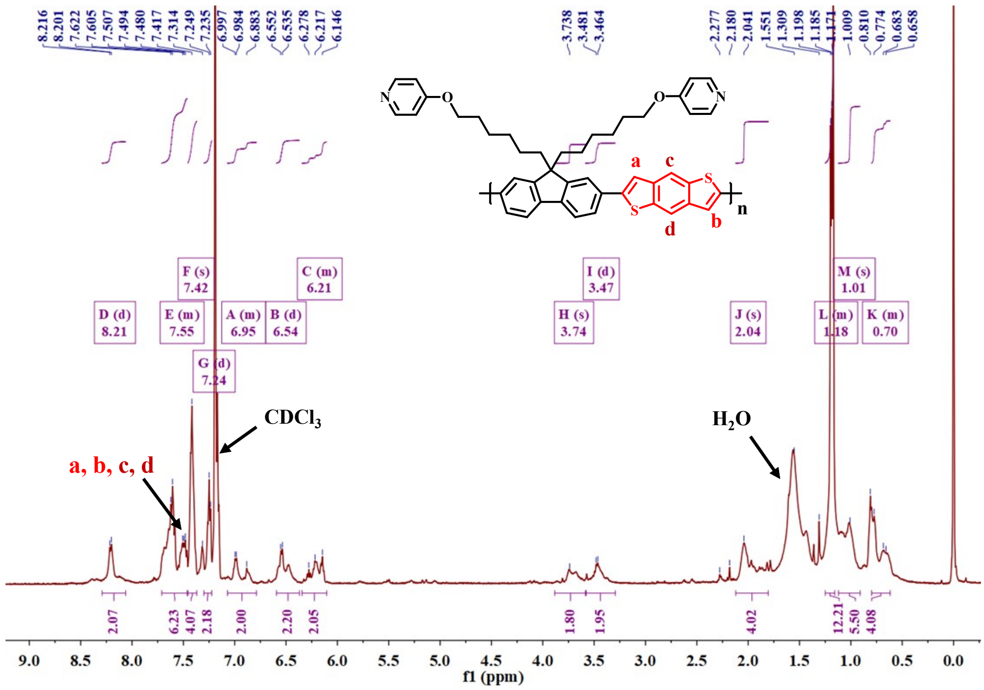

Fig. S3 The ^{1}H NMR of PF-BDT. $CDCl_3$ is used as the deuterium reagent.

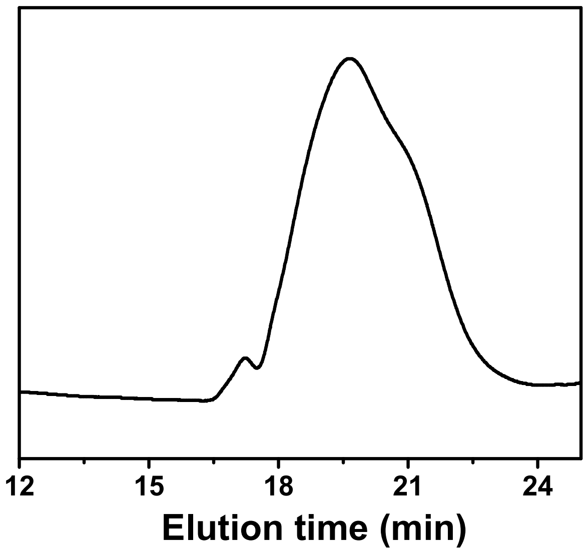

Fig. S4 GPC trace of PF-BDT. THF is used as the eluent.

Table S1. UV-vis absorption and electrochemical properties of the three CILs.

CIL	λ_{onset} (nm)	$^{a}E_g^{opt}$ (eV)	$^{b}E_{HOMO}$ (eV)	$^{b}E_{LUMO}$ (eV)
PF-TT	498	2.49	-5.46	-3.46
PF-BDT	480	2.58	-5.51	-3.49
PDINO	623	1.99	-5.34	-3.25

$^{a}E_g^{opt} = 1240/\lambda_{onset}$

$^{b}E_{HOMO} = -e(E_{onset,ox} + 4.37\ eV)$

$^{b}E_{LUMO} = -e(E_{onset,red} + 4.37\ eV)$

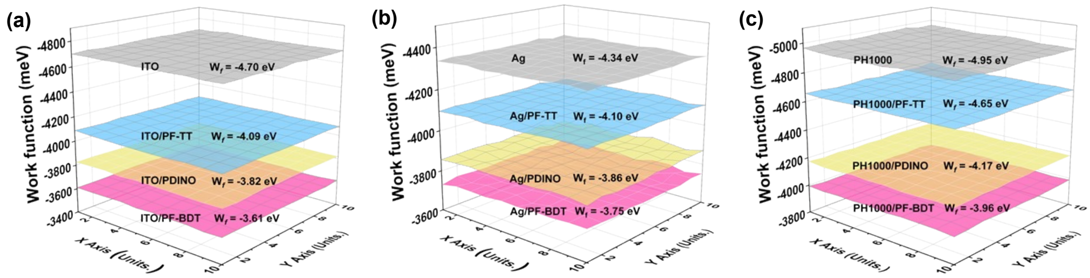

Fig. S5 Source data for the measured W_f of the conducting materials (ITO, Ag, PH1000) with and without the surface modifiers.

Table S2. W_f changes of ITO, Ag and PH1000 modified with and without different CIL.

	Bare	PF-TT	PF-BDT	PDINO
ITO	-4.70±0.004 eV	-4.08±0.005 eV	-3.61±0.005 eV	-3.82±0.004 eV
Ag	-4.34±0.004 eV	-4.10±0.004 eV	-3.75±0.006 eV	-3.86±0.006 eV
PEDOT:PSS (PH1000)	-4.95±0.009 eV	-4.65±0.004 eV	-3.99±0.004 eV	-4.17±0.004 eV

The ± refers to the standard deviation from 100 values.

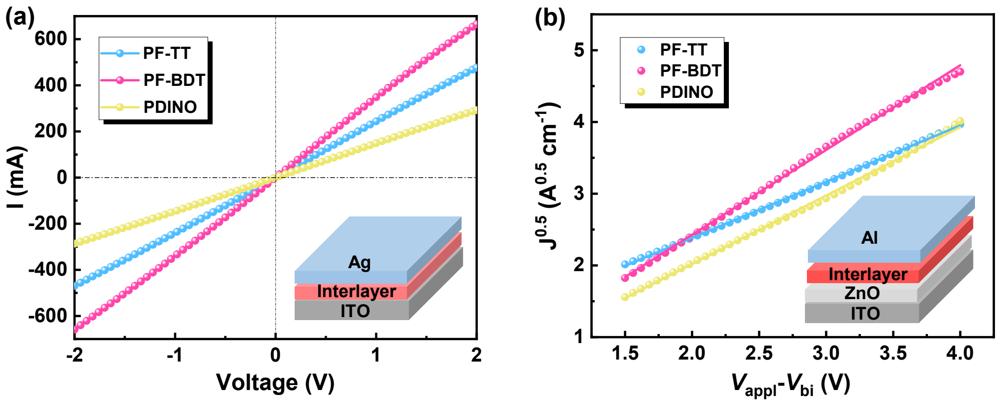

Fig. S6 (a) Conductivity and **(b)** electron mobility of the devices with a structure in the inset based on different interlayer.

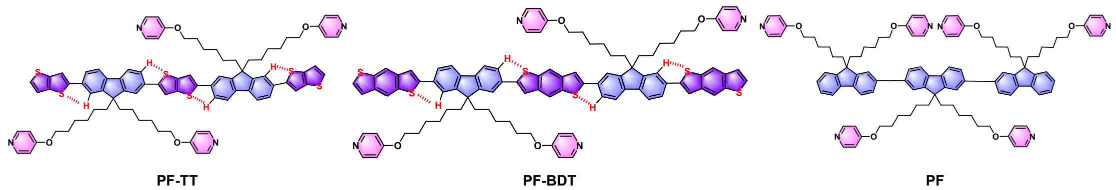

Fig. S7 Chemical structure formula of PF, PF-TT and PF-BDT used for DFT calculations.

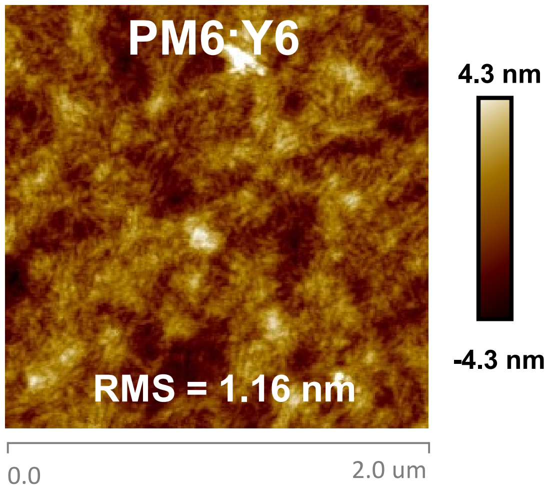

Fig. S8 AFM image of the bare PM6:Y6 active layer film.

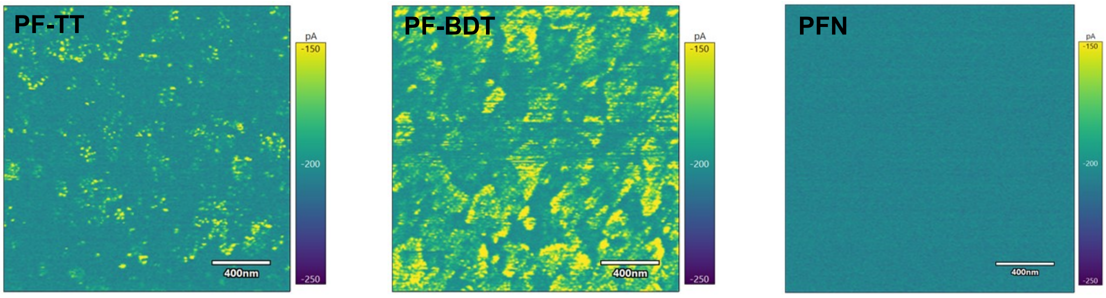

Fig. S9 The current-sensing AFM (C-AFM) of the PF-TT, PF-BDT and PFN thin films. The thickness of the films is ~50 nm.

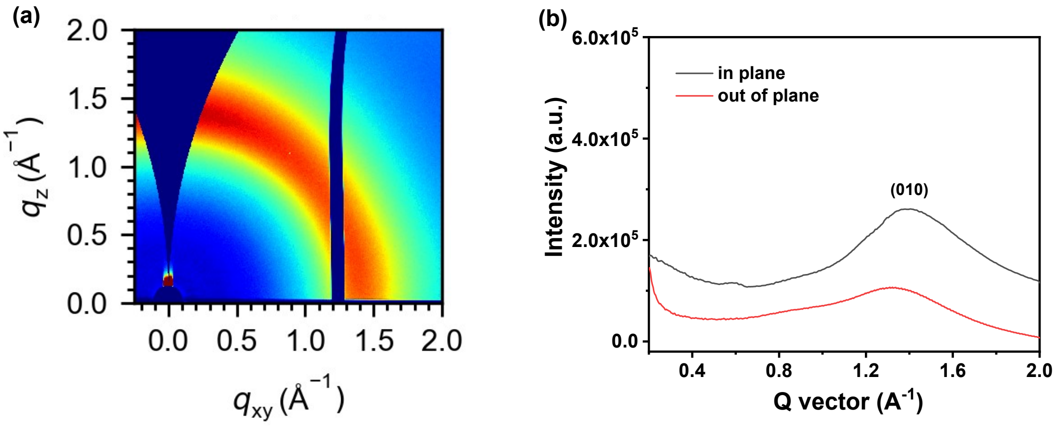

Fig. S10 (a) 2D GIWAXS images and **(b)** 1D GIWAXS line curves of the PFN film used for comparison.

Table S3. Molecular orientation and crystallinity information of 2D GIWAXS.

CIL	010 direction	Peak (Å^{-1})	FWHM (Å^{-1})^{a}	*d*-spacing (Å)	Coherence length (Å)
PF-TT	(*IP*)	1.44	0.39	4.36	14.33
	(*OOP*)	1.41	0.33	4.45	16.93
PF-BDT	(*IP*)	1.35	0.37	4.65	15.11
	(*OOP*)	1.34	0.42	4.68	13.30
PFN	(*IP*)	1.40	0.57	4.48	9.80
	(*OOP*)	1.31	0.54	4.79	10.35

[a]FWHM = full-width at half-maximum.

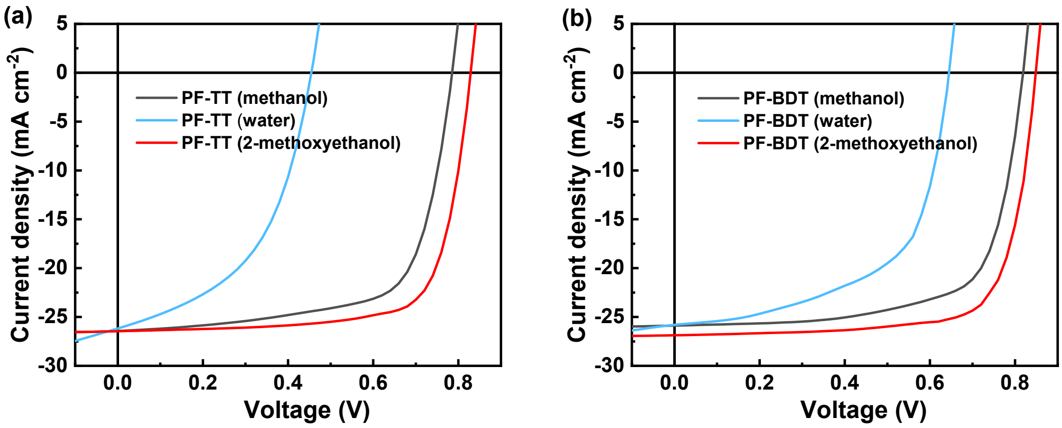

Fig. S11 *J-V* curves of PM6:Y6-based devices with PF-TT and PF-BDT as CIL derived from methanol, water or 2-methoxyethanol, respectively.

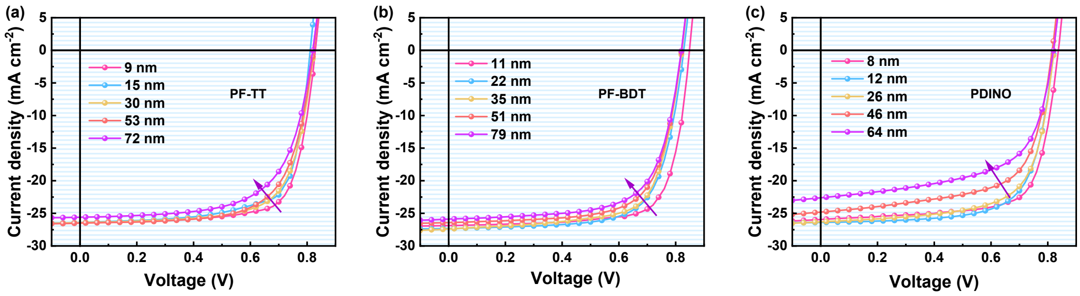

Fig. S12 *J-V* curves of PM6:Y6-based devices with **(a)** PF-TT, **(b)** PF-BDT and **(c)** PDINO at different film thickness.

Table S4. Parameters of PM6:Y6-based devices with different concentrations of PF-TT, PF-BDT and PDINO. The thickness of the films are determined by a step profiler.

CIL	Concentration	Thickness	V_{OC} (V)	J_{SC} (mA cm^{-2})	FF (%)	PCE (%)
PF-TT	1 mg/mL	9 nm	0.83	26.46	74.08	16.27
	2 mg/mL	15 nm	0.82	26.42	71.63	15.52
	3 mg/mL	30 nm	0.82	26.41	69.92	15.30
	4 mg/mL	53 nm	0.82	26.50	67.99	14.82
	5 mg/mL	72 nm	0.82	25.60	64.99	13.64
PF-BDT	1 mg/mL	11 nm	0.85	26.88	74.80	17.09
	2 mg/mL	22 nm	0.83	27.32	70.71	16.15
	3 mg/mL	35 nm	0.82	27.39	70.36	15.87
	4 mg/mL	51 nm	0.82	26.42	69.39	15.05
	5 mg/mL	79 nm	0.82	25.89	68.16	14.47
PDINO	1 mg/mL	8 nm	0.84	25.94	72.63	15.79
	2 mg/mL	12 nm	0.82	26.40	70.41	15.26
	3 mg/mL	26 nm	0.82	26.30	68.31	14.75
	4 mg/mL	46 nm	0.82	24.81	64.91	13.13
	5 mg/mL	64 nm	0.82	22.61	61.03	11.31

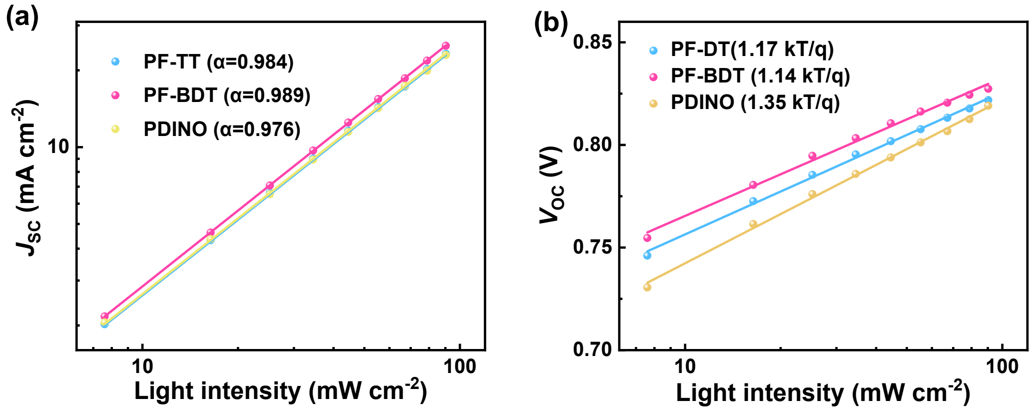

Fig. S13 The dependence of **(a)** J_{SC} and **(b)** V_{OC} of the OSCs on the light intensity. They can be described according to the equations of $J_{SC} \propto P_{light}^{\alpha}$ (α represents the degree of recombination) and $V_{OC} \propto nkT/q\ln P_{light}$ (k, T and q represent Boltzmann constant, temperature in Kelvin and elementary charge), respectively.

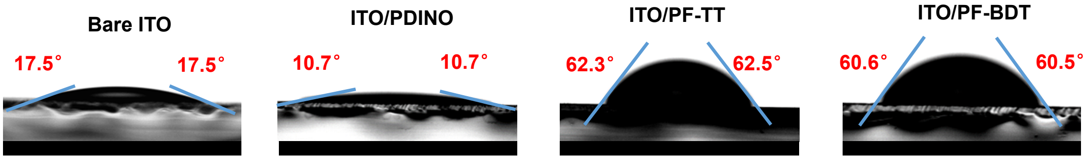

Fig. S14 The contact angle measurements of different films to deionized water.

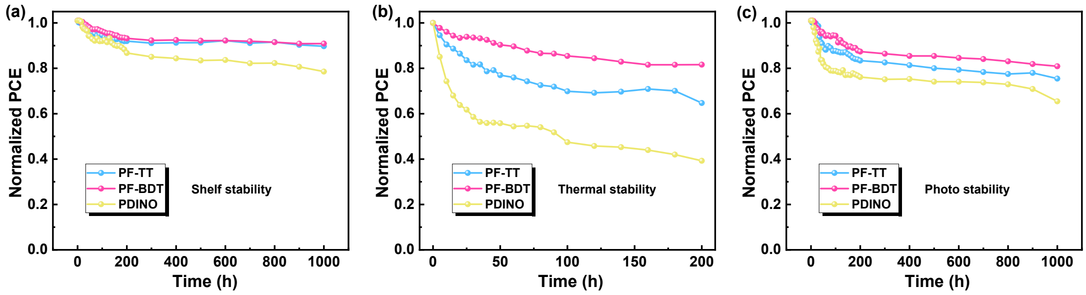

Fig. S15 Normalized PCE degradation trend of the optimized non-fullerene OSCs with PF-TT, PF-BDT, and PDINO as CIL under different conditions: **(a)** stored in a N_2-filled glove-box (shelf stability), **(b)** continuously heated at 85 °C (thermal stability) and **(c)** exposed under the illumination of AM 1.5G, 100 mW/cm^2 with a white LED light in the glove box (photo stability).

Table S5. A summary of the photovoltaic parameters of reported non-fullerene OSCs using thick CILs (>30 nm) and the results in this work (Corresponding to **Fig. 6d**). The thickness-scaling loss of PCE is defined as ΔPCE/Δt×100% (%/nm).

Active Layer	CIL	Thickness (nm)	V_{OC} (V)	J_{SC} (mA·cm^{-2})	FF (%)	PCE (%)	thickness-scaling loss of PCE (%/nm)	Ref
PTB7-Th: N2200	PFN-2TNDI	5	0.92	16.59	70	10.8	4.64%	1
		33	0.92	15.18	69	9.5		
PTB7-Th: IEICO-4F	P2G	5	0.71	23.6	62.2	10.5	3.76%	2
		35	0.71	20.9	62.7	9.37		
PBDB-T: IT-M	PDI-z	12	0.94	16.12	74.17	11.23	7.89%	3
		40	0.90	15.01	66.78	9.02		
PBDB-T: ITIC	PMI-TPP	13	0.87	15.90	69	9.56	0.45%	4
		55	0.88	15.25	69	9.37		
PBDTS-TDZ: IT-4F	ATF	5	0.88	18.83	68.2	11.30	22.56%	5
		50	0.53	5.10	42.5	1.15		
	STF	5	0.89	19.32	70.5	12.12	8.76%	
		50	0.87	16.02	58.7	8.18		
	OTF	5	0.88	19.89	74.6	13.21	8.22%	
		50	0.88	17.18	62.9	9.51		
PBDB-2Cl: ITIC-2F	PNDT	20	0.88	20.77	74.63	13.33	2.5%	6
		50	0.87	19.58	74.88	12.58		
	PNDTOO	10	0.85	21.10	69.14	12.44	1.4%	
		50	0.87	19.97	74.29	13.00		
PM6:IT-4F	NDI-N	5	0.86	20.8	76.0	13.5	7.33%	7
		50	0.86	15.9	74.0	10.2		
PTQ10: IDIC-2F	PDINO-G	5	0.91	19.09	74.87	13.01	1.52%	8
		32	0.91	18.76	73.72	12.60		
PM6: Y6	PEDETA-DBO	5	0.835	26.85	72.39	16.57	12.64%	9
		30	0.816	24.22	65.83	13.41		
PM6:Y6	PDINO	9	0.843	25.54	74.81	15.46	12.47%	10
		39	0.834	19.76	71.12	11.72		
PM6:Y6	NTA	11	0.849	26.72	74.3	16.86	12.88%	11
		35	0.822	25.04	66.9	13.77		
PM6:Y6	PDINOH	10	0.851	26.40	78.32	17.60	7.28%	12
		53	0.830	24.77	70.39	14.47		
PM6:Y6	NEA	8	0.873	24.94	69.1	15.04	12.07%	13
		36	0.835	25.38	55.0	11.66		
PM6:Y6	PTPAPDINO	14	0.83	25.49	74.10	13.01	2.93%	14
		28	0.83	22.96	67.81	12.60		
PM6:Y6	TOASiW12	8	0.85	25.42	74.7	16.14	18.56%	15
		33	0.845	24.24	56.2	11.50		

PM6:Y6	PBI-2P	4	0.840	25.94	72.56	15.79	13.64%	16
		32	0.840	24.47	58.20	11.97		
PM6: Y6C12	PDIN-EH	7	0.82	23.1	55.7	11.0	1.61%	17
		38	0.83	22.5	54.8	10.5		
PM6:Y6	PDINN-2F	10	0.84	26.31	76.1	16.82	7.16%	18
		55	0.80	24.88	68.3	13.60		
PM6:Y6	NDI-NI	8	0.84	25.74	73.93	16.06	2.38%	19
		37	0.84	24.95	73.27	15.37		
PM6:Y6	PNDIT-F3N-Br	30	0.83	26.12	74.39	16.18	4.3%	20
		60	0.83	25.17	71.07	14.89		
PM6:Y6	SiNcTI-Br	4	0.860	26.8	76.0	17.5	6.88%	21
		36	0.851	25.1	71.3	15.3		
PM6:Y6	NDI-DABC	19	0.857	26.38	77.25	17.44	2.27%	22
		41	0.849	26.28	75.86	16.94		
BTR-Cl:Y6	PDINN: 7%DOH	10	0.852	25.36	73.55	15.88	7.28%	23
		50	0.830	22.11	70.68	12.97		
PM6: BTP-eC9	t-PyPDINO	10	0.843	27.61	75.09	17.49	3.29%	24
		45	0.840	26.69	72.89	16.34		
	t-PyPDINBr	6	0.833	27.70	74.31	17.15	5.68%	
		53	0.827	24.10	72.59	14.48		
PM6:BTP-eC9	**PF-BDT**	**11**	**0.85**	**27.41**	**79.28**	**18.47**	**7.52%**	**This Work**
		53	**0.82**	**26.48**	**70.05**	**15.31**		

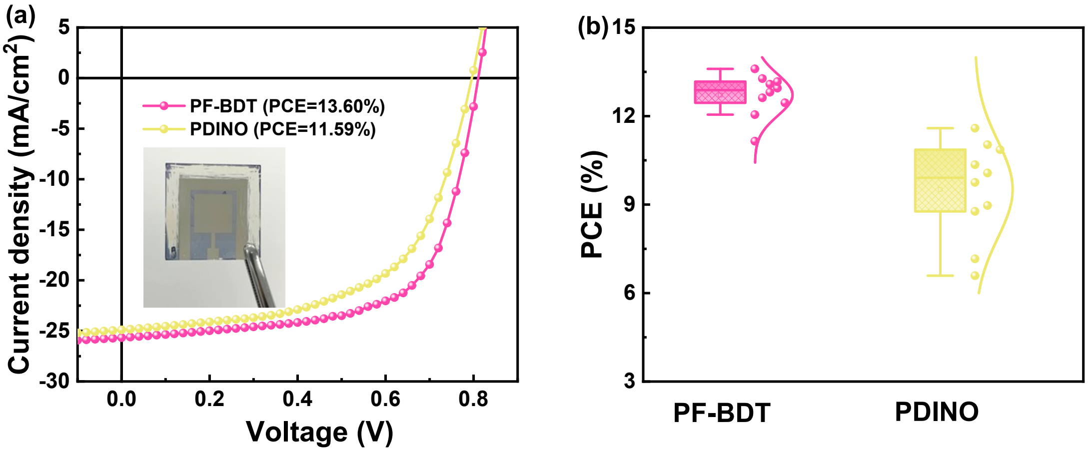

Fig. S16 (a) *J-V* curves of the printable PM6:BTP-eC9-based non-fullerene OSCs with blade-coated PF-BDT (~60 nm) and PDINO (~50 nm) CIL. A physical map is inserted in the inset and the aperture area is 1 cm^2. **(b)** PCE statistics distribution of 10 individual cells.

References

1. Sun, C.; Wu, Z., Hu, Z.; Xiao, J.; Zhao, W.; Li, H.-W.; Li, Q.-Y.; Tsang, S.-W.; Xu, Y.-X.; Zhang, K.; Yip, H.-L.; Hou, J.; Huang, F.; Y. Cao. Interface Design for High-efficiency Non-fullerene Polymer Solar Cells. *Energy Environ. Sci.* **2017**, *10*, 1784-1791.
2. Sharma, A.; Singh, S.; Song, X.; Villalva, D. R.; Troughton, J.; Corzo, D.; Toppare, L.; Gunbas, G.; Schroeder, B. C.; Baran, D. A Nonionic Alcohol Soluble Polymer Cathode Interlayer Enables Efficient Organic and Perovskite Solar Cells. *Chem. Mater.* **2021**, *33*, 8602-8611.
3. Xu, R.; Zhang, K.; Liu, X.; Jin, Y.; Jiang, X. F.; Xu, Q. H.; Huang, F.; Cao, Y. Alkali Salt-doped Highly Transparent and Thickness-insensitive Electron-transport Layer for High-performance Polymer Solar Cell. *ACS Appl. Mater. Interfaces*, **2018**, *10*, 1939-1947.
4. Qin, R.; Guo, D.; Hu, L.; Liu, Z.; Yang, J.; Liu, H.; Jiang, L.; Jiang, Y. Organic Solar Cells' Efficiency Enhanced by Perylene Monoimide Phosphorus Salt Cathode Interfacial Layer. *Energy Technol*., **2020**, *8*, 2000072.
5. Wang, S.; Li, Z.; Xu, X.; Zhang, M.; Zhang, G.; Li, Y.; Peng, Q. Self-doping Small Molecular Conjugated Electrolytes Enabled by n-Type Side Chains for Highly Efficient Non-fullerene Polymer Solar Cells. *J. Mater. Chem. A* **2018**, *6*, 22503-22507.
6. Hu, Z.; Chen, Z.; Jing, J.; Liang, Y.; Bai, Y.; Liu, X.; Huang, F.; Cao, Y. Direct Arylation Polycondensed Conjugated Polyelectrolytes as Universal Electron Transport Layers for Highly Efficient Polymer Solar Cells. *J. Mater. Chem. C* **2020**, *8*, 15158-15167.
7. Kang, Q.; Ye, L.; Xu, B.; An, C.; Stuard, S. J.; Zhang, S.; Yao, H.; Ade, H.; Hou, J. A Printable Organic Cathode Interlayer Enables over 13% Efficiency for 1-cm2 Organic Solar Cells. *Joule* **2019**, *3*, 227-239.
8. Pan, F.; Sun, C.; Li, Y.; Tang, D.; Zou, Y.; Li, X.; Bai, S.; Wei, X.; Lv, M.; Chen, X.; Li, Y. Solution-processable n-Doped Graphene-containing Cathode Interfacial Materials for High-performance Organic Solar Cells. *Energy Environ. Sci.* **2019**, *12*, 3400-3411.
9. Yu, Y.; Tao, W.; Wang, L.; Tao, Y. D.; Peng, Z.; Zheng, X.; Xiang, C.; Zhao, B.; Li C.-Z.; Tan, S. Non-conjugated Electrolytes as Thickness-insensitive Interfacial Layers for High-Performance Organic Solar Cells. *J. Mater. Chem. A*, **2021**, *9*, 22926-22933.

10. Cai, C.; Yao, J.; Chen, L.; Yuan, Z.; Zhang, Z. G.; Hu, Y.; Zhao, X.; Zhang.; Y. Chen.; Li, Y. Silicon Naphthalocyanine Tetraimides: Cathode Interlayer Materials for Highly Efficient Organic Solar Cells. *Angew. Chem., Int. Ed.* **2021**, *60*, 19053-19057.
11. Zhao, Y.; Liu, X.; Jing, X.; Liu, S.; Liu, H.; Liu, Y.; Yu, L.; Dai S.; Sun, M. Multi-armed Imide-based Molecules Promote Interfacial Charge Transfer for Efficient Organic Solar Cells. *Chem. Eng. J.* **2022**, *441*, 135894.
12. Zi, M.; Chen, X.; Tan, S.; Weng, C.; Zhao, B. Organic Solar Cells with Efficiency of 17.6% and Fill Factor of 78.3% based on Perylene-diimide Derivative as Cathode Interface Layer. *Chem. Eng. J.* **2022**, *443*, 136455.
13. Zhao, Y.; Liu, Y.; Liu, X.; Kang, X.; Yu, L.; Dai, S.; Sun, M. Aminonaphthalimide-Based Molecular Cathode Interlayers for As-Cast Organic Solar Cells. *Chem. Sus. Chem*, **2021**, 14, 4783-4792.
14. Zhou, D.; You, W.; Yang, F.; Chen, R.; Xu, H.; Tong, Y.; Hu, B.; Hu, Lin.; Xie, Y.; Chen, L. N-type Self-doped Hyperbranched Conjugated Polyelectrolyte as Electron Transport Layer for Efficient Nonfullerene Organic Solar Cells. *ACS Appl. Mater. Interfaces*, **2021**, *13*, 50187-50196.
15. Qiu, J.; Zhang, Y.; Liu, Y.; Liu, H.; Xia, D.; Yang, F.; Zhao, C.; Li, W.; Wu. L.; Li, F. Surfactant-Encapsulated Polyoxometalate Complex as a Cathode Interlayer for Nonfullerene Polymer Solar Cells. *CCS Chem*. **2022**, *4*, 975-986.
16. Wen, X.; Zhang, Y.; Xie, G.; Rausch, R.; Tang, N.; Zheng, N.; Liu, L.; Würthner, F.; Xie, Z. Phenol-Functionalized Perylene Bisimides as Amine-Free Electron Transporting Interlayers for Stable Nonfullerene Organic Solar Cells. *Adv. Funct. Mater.* **2022**, *32*, 2111706.
17. Hoff, A.; Gasonoo, A.; Pahlevani, M.; Welch, G. C. An Alcohol-Soluble N-Annulated Perylene Diimide Cathode Interlayer for Air-Processed, Slot-Die Coated Organic Photovoltaic Devices and Large-Area Modules. *Sol. RRL*, **2022**, *6*, 2200691.
18. Yao, J.; Ding, S.; Zhang, R.; Bai, Y.; Zhou, Q.; Meng, L.; Solano, E.; Steele J. A.; Roeffaers, M. B. J.; Gao, F.; Zhang, Z. G.; Li, Y. Fluorinated Perylene-Diimides: Cathode Interlayers Facilitating Carrier Collection for High-Performance Organic Solar Cells. *Adv. Mater*. **2022**, 34, 2203690.

19. Liu, M.; Fan, P.; Hu, Q.; Russell, T. P.; Liu, Y. Naphthalene-Diimide-based Ionenes as Universal Interlayers for Efficient Organic Solar Cells. *Angew. Chem. Int. Ed.* **2020**, *59*, 18131-18135.
20. Tian, L.; Jing, J.; Tang, H.; Liang, Y.; Hu, Z.; Rafiq, M.; Huang, F.; Cao, Y. Aldol Condensation-Polymerized n-Doped Conjugated Polyelectrolytes for High-Performance Nonfullerene Polymer Solar Cells. *Sol. RRL,* **2020**, *5*, 2000523.
21. Qin, Y.; Chang, Y.; Zhu, X.; Gu, X.; Guo, L.; Zhang, Y.; Wang, Q.; Zhang, J.; Zhang, X.; Liu, X.; Lu, K.; Zhou, E.; Wei, Z.; Sun, X. 18.4% Efficiency Achieved by the Cathode Interface Engineering in Non-fullerene Polymer Solar Cells. *Nano Today,* **2021**, *41*, 101289
22. You, Z.; Song, Y.; Liu, W.; Wang, W.; Zhu, C.; Duan, Y.; Liu, Y. Diazabicyclic Electroactive Ionenes for Efficient and Stable Organic Solar Cells. *Angew. Chem. Int. Ed.* **2023**, *62*, e202302538
23. Cao, L.; Du, X.; Li, X.; He, Z.; Lin, H.; Zheng, C.; Yang, G.; Chen, Z.; Tao, S. Hydrogen Bond-Induced Cathode Engineering Enables Binary All-Small-Molecule Organic Solar Cells with 15.88% Efficiency and Enhanced Thermostability. *Sol. RRL*, **2022**, *6*, 2200477.
24. Sun, W. J.; Wang, Y. T.; Zhang, Y.; Sun, B.; Zhang, Z. Q.; Xiao, M. J.; Li, X. Y.; Huo, Y.; Xin, J.; Zhu, Q.; Ma, W.; Zhang, H. L. A Cathode Interface Layer Based on 4, 5, 9, 10-Pyrene Diimide for Highly Efficient Binary Organic Solar Cells. *Angew. Chem. Int. Ed.* **2022**, *61*, e202208383.